High-throughput study of alpha-synuclein expression in yeast using microfluidics for control of local cellular microenvironment

Patrícia Rosa,[1,a)] Sandra Tenreiro,[2,a)] Virginia Chu,[1] Tiago F. Outeiro,[2,3] and João Pedro Conde[1,4]
[1]*INESC Microsistemas e Nanotecnologias (INESC MN) and IN-Institute of Nanoscience and Nanotechnology, Rua Alves Redol, 9, Lisbon 1000-029, Portugal*
[2]*Instituto de Medicina Molecular, Faculdade de Medicina da Universidade de Lisboa Av. Prof. Egas Moniz, 1649-028 Lisboa, Portugal*
[3]*Department of Neurodegeneration and Restaurative Research, University Medizin Goettingen, Goettingen, Germany*
[4]*Department of Bioengineering, Instituto Superior Técnico, Av Rovisco Pais 1, Lisbon 1049-001, Portugal*

(Received 24 October 2011; accepted 12 January 2012; published online 9 February 2012)

Microfluidics is an emerging technology which allows the miniaturization, integration, and automation of fluid handling processes. Microfluidic systems offer low sample consumption, significantly reduced processing time, and the prospect of massive parallelization. A microfluidic platform was developed for the control of the soluble cellular microenvironment of *Saccharomyces cerevisiae* cells, which enabled high-throughput monitoring of the controlled expression of alpha-synuclein (aSyn), a protein involved in Parkinson's disease. Y-shaped structures were fabricated using particle desorption mass spectrometry-based soft-lithography techniques to generate biomolecular gradients along a microchannel. Cell traps integrated along the microchannel allowed the positioning and monitoring of cells in precise locations, where different, well-controlled chemical environments were established. *S. cerevisiae* cells genetically engineered to encode the fusion protein aSyn-GFP (green fluorescent protein) under the control of *GAL1*, a galactose inducible promoter, were loaded in the microfluidic structure. A galactose concentration gradient was established in the channel and a time-dependent aSyn-GFP expression was obtained as a function of the positioning of cells along the galactose gradient. Our results demonstrate the applicability of this microfluidic platform to the spatio-temporal control of cellular microenvironment and open a range of possibilities for the study of cellular processes based on single-cell analysis. © *2012 American Institute of Physics*. [doi:10.1063/1.3683161]

I. INTRODUCTION

Microfluidics is a promising technology for miniaturizing and parallelizing fluid-addressable investigation of stimulus-response relationships and spatiotemporal dynamics in cellular behavior (cell-chips). The effects of scale in microfluidic structures lead to new phenomena and allow novel applications that are not accessible to classical liquid handling platforms. In particular, laminar flow enables the formation of highly controlled flow patterns and concentration profiles, the ability to match device dimensions with characteristic cellular dimensions, the potential to achieve both high-speed serial processing and massive parallelization, and the reduction of cell and reagent consumption. These emerging experimental devices have the potential to rapidly probe cellular genomic and proteomic responses, to discover the

[a)]P. Rosa and S. Tenreiro contributed equally to this work.

biochemical signals that affect cellular function, and to probe the complex and dynamic relationships between cells and their microenvironment.

In one particular implementation of a cell-chip platform, which was used in this work, cells are introduced and allowed to attach to a cell culture module. A microfluidic gradient generator is integrated upstream to the cell culture module. The basic unit operation in this type of platform is the contacting of at least two liquid streams at a microfluidic channel junction, allowing diffusion-controlled mixing at the interface. A gene expression inducer is inserted in one of the liquid streams and then delivered to individual cell culture chambers. The expression dynamics of the gene of interest tagged with green fluorescent protein (GFP) can be extracted using fluorescence imaging.[1–4] This platform is of particular relevance since a variety of conditions can be screened simultaneously and thus affords efficient exploration of a wide parameter space for molecular stimulation of cells.

There are several microfluidic techniques for cell attachment, which can be classified as cell immobilization on a surface or as contactless cell trapping. The former comprises chemical and hydrodynamic trapping. Optical, dielectrophoretic, acoustic, and magnetic trapping belong to the latter. Cell encapsulation in a polymer is regarded as being situated in between.[4] In this work, hydrodynamic trapping was employed, which is based on the use of variations of surface topography to separate particles from a flow and immobilize them on certain sites of the chip, providing a passage for the fluid only. Mechanical obstacles or barriers with dimensions appropriate to the size of the cells to be captured must be used. Regions of low shear stress are appropriate for retaining particles at rest next to a moving fluid. Among the advantages in using hydrodynamic trapping are fast cell immobilization, simplicity of the method, and no requirements for peripheral instrumentation. The main difficulty lies in achieving precision in cell attachment: in some cases, array sites may remain empty; in other cases, aggregates can be trapped instead of single particles.[4]

Gradient generation in microfluidics has been used to study biological signaling phenomena including development and differentiation of cells,[5] immune response,[6] and cancer metastasis.[7] The generation of a controllable gradient can also be integrated into cell-based drug testing schemes to investigate the concentration-dependent cellular responses to drug concentrations.[8] Y-shaped parallel flow gradient generators are conceptually the simplest and are based on two or more microchannels that join into a single microchannel. In practical terms, these have been utilized to combine dissimilar fluid streams to create combinatorial mixtures of different chemicals and perform biological assays. These devices generate steady-state gradients, which are reproducible and can be characterized quantitatively. They also have simple designs, which allow easy fabrication and modeling. Cell growth and cellular processes can be visualized within the microchannel and can be correlated with specific gradient characteristics due to the temporal stability of the gradient. The perfusion ensures the continuous application of confining mechanical forces and also the continuous supply of nutrients and cell waste removal, allowing cells to be maintained for long periods in culture. By adjusting the inlet flow rates and solution concentrations, the position and shape of the gradient can be modulated dynamically. Y-shaped gradient generators also have limitations in that they can only generate single-solute gradients, and the gradients are confined to a single axis perpendicular to the direction of fluid flow, precluding more complex multifactor gradient environments.[9] Recently, a microfluidic platform was developed to generate concentration gradients of 6-hydroxydopamine to trigger a process of neuronal apoptosis in immobilized pheochromocytoma PC12 neuronal cell line.[10]

The biological model used in this work was *Saccharomyces cerevisiae* genetically modified to express human alpha-synuclein (aSyn) with a C-terminal fusion with the green fluorescent protein GFP under the control of the *GAL1* inducible promoter.[11] ASyn is a protein involved in Parkinson's disease (PD) and other neurodegenerative disorders collectively referred to as synucleinopathies.[12] This protein was first identified as the major constituent of Lewy bodies, which consist of cellular inclusions that are the pathological hallmark of PD.[12] After that, several studies have shown that missense mutations in the aSyn gene (A53T, A30P, E46K), as well as duplication or triplication of the locus, cause familial cases of PD [reviewed in Ref. 13]. A *S. cerevisiae* model was developed to uncover and establish basic aspects of both normal and abnormal aSyn biology.[11] Namely, it was observed that when expressed in yeast cells, aSyn

presents a high intrinsic selectivity for cellular membranes. However, aSyn point mutants such as A53T and A30P altered aSyn distribution. Another aspect was that when aSyn overexpression occurred, the protein showed cytoplasmic inclusions, reducing its membrane localization and inhibiting cell growth.[11] ASyn is differentially expressed throughout the brain and throughout the organism.[14,15] Therefore, single cell analysis is essential to better understand the molecular effects of different levels of aSyn and, ultimately, to determine why some cell types appear more sensitive to its accumulation.

In this study, yeast cells harboring double genome insertions of the human gene encoding aSyn with a GFP fusion and, under the regulation of a galactose-inducible promoter, were hydrodynamically trapped in a particle desorption mass spectrometry (Polydimethylsiloxane (PDMS))-based microfluidic channel. This cell-culture module was integrated with a Y-shaped parallel flow gradient generator to provide spatial and temporal control of the local biochemical environment of a group of cells. The cells were exposed to a gradient of galactose, and the expression of the protein of interest was monitored via GFP fluorescence. The results obtained demonstrate that a range of aSyn expression levels, with a direct relation to the galactose gradient generated, can be obtained with the developed microfluidic platform The classical techniques, such as flow-cytometry or fluorescence microscopy, are powerful but can only provide a global overview of the whole population of cells at a given time. In contrast, the microfluidic platform developed in this study enables the growth of yeast cells under controlled conditions and the monitoring of the spatio-temporal distribution of aSyn in individual yeast cells. Moreover, this enables the direct correlation of the levels of aSyn expression with the molecular effects induced, such as cell viability, accumulation of reactive oxygen species, aSyn distribution and aggregation, and effects on trafficking.

II. MATERIALS AND METHODS

A. Microfluidic structure fabrication

The microfluidic structures were fabricated using PDMS soft-lithography.[16,17] The mold material was positive photoresist PFR 7790G 27cP from JSR Micro. Before resist coating, the surface of the glass substrate was treated with hexamethyldisilizane (HMDS) for 30 min in a vapor priming step. Four consecutive steps of resist spin coating and baking were repeated to achieve a total mold thickness of 6 μm. Patterning of the resist layer was performed in a Direct Writer Laser (DWL) lithography system using 422 nm wavelength light. After development, the mold was baked at 120 °C for 5 h.

To produce the PDMS replica, SylgardTM 184 (Dow Corning) silicone was poured over the mold and was baked at 70 °C for 2 h. After curing, a needle with a blunt tip was used to make the fluid connection access holes. The PDMS is then peeled from the mold and cleaned with acetone and IPA and dried with compressed air. The PDMS replica was irreversibly sealed to a glass slide, with thickness of 170 μm, using either a UV-ozone (UVO) or a corona discharge for surface activation. Figure 1 shows schematically the fabrication process flow.

Figure 2 shows the microfluidic device fabricated as described above and following the insertion of metal catheters (Instech Solomon, d = 0.8 mm) into the access holes in the PDMS, sealing with silicone, and coupling to plastic tubes. The overall structure is Y-shaped with two inlets as illustrated in Figure 2(b). The main microchannel is 20 mm long, 200 μm wide, and 6 μm high. At periodic distances along the main microchannel, pairs of "U"-shaped cell traps are defined, together with a pillar that helps to prevent sagging of the top of the microchannel [Fig. 2(c)]. A ruler is photolithographically defined along the side of the channel to facilitate the identification of a particular set of traps when using the optical microscope [Fig. 2(c)]. Figure 2(d) indicates the critical dimensions of the traps and their location with respect to each other and to the sides of the channel.

B. Generation of stable gradients and further validation by fluorescence microscopy

COMSOL Multiphysics® 3.5 software was used to simulate the gradient generation in the "Y"-shaped microfluidic structure. To validate the simulation results water was inserted in one

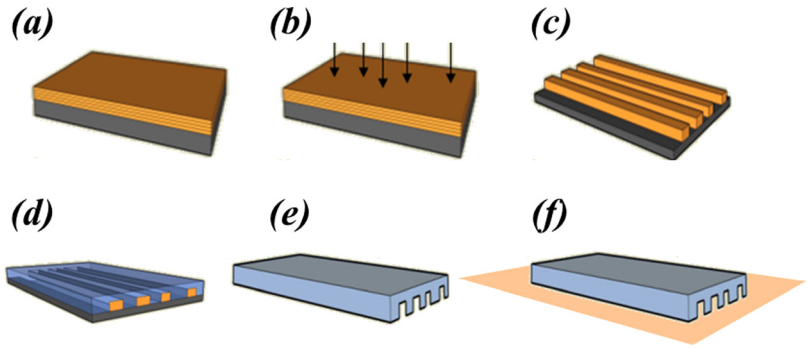

FIG. 1. Fabrication process flow of the PDMS microchannels—Mold definition involves: (a) Spin-coating of 4 layers of positive photoresist with a total thickness of 6 μm; (b) photolithographic patterning of the photoresist; and finally (c) development of the resist to form the mold pattern. To produce the microchannels: (d) PDMS is poured onto the mold and baked; (e) then peeled from the mold; and (f) sealed to the glass slide following a surface treatment.

inlet channel and a fluorescein isothiocyanate (FITC, Sigma-Aldrich®) solution (25 μM FITC in water) in the other. The pumping of the solutions was performed using syringe pumps (NE-300, SyringePump.com). The syringes (U-100 Insulin, 1 mL Codan) were connected to the microfluidic inlets using polytethlene tubes (Instech Solomon). The outlet was connected via a polyethylene tube to a waste reservoir. FITC fluorescence was monitored using a DMLM model fluorescence microscope from Leica Microsystems Ltd. with digital color camera Leica DFC300 FX. Microscope and digital camera were controlled via JASC Paint Shop Pro® and

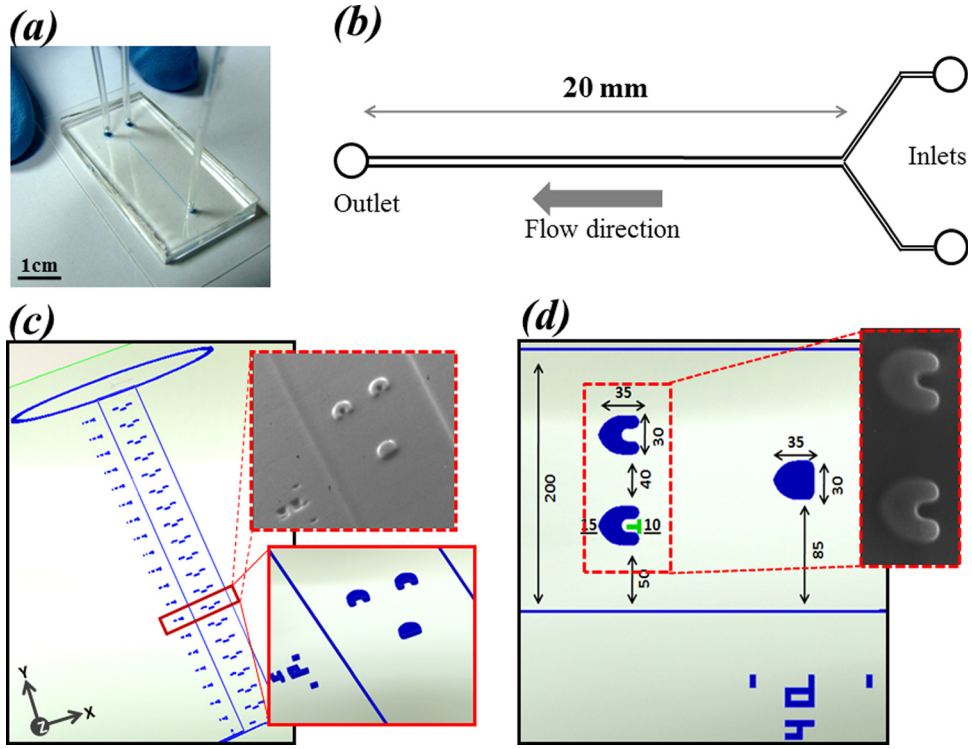

FIG. 2. Microfluidic device: (a) Photograph of the PDMS chip on a glass substrate. (b) The Y-shaped structure is composed of one flow channel with incorporated cell traps with two inlets, one outlet and ruler along the length of the microchannel; the arrow shows the flow direction as indicated in the figure. (c) Scanning electron microscope images show details of PDMS cell traps. (d) Dimensions of microchannel and traps. All dimensions are in μm; the height of the microchannel, traps, and ruler is 6 μm. Insets represent enlarged images or scanning electron microscope images of PDMS cell traps in the boxed regions.

CAMSTUDIO® software. A field of view (FOV) of 320 × magnification was scanned along the microchannel with the aid of the scale defined along the length of the microchannel and bright field, and fluorescence images were obtained. An exposure time of 540 ms was used for fluorescence images. The micrographs were analyzed using IMAGEJ® software.

C. Cell media and growth conditions

The *S. cerevisiae* strain used was VSY72 (can1-100 his3-11 15 leu2-3 112 GAL1pr-SNCA(WT)-GFP::TRP1 GAL1pr-SNCA(WT)-GFP::URA3 ade2-1, a kind gift from Prof. Paul Muchowski, Gladstone Institute for Neurological Disease, UCSF, USA). On this strain, two copies of the SNCA human gene, which encodes aSyn, having a C-terminal fusion with GFP and under the control of the *GAL1* inducible promoter, were inserted in the genome. The cells were first grown at 30 °C for 24 h, in synthetic complete (SC) raffinose liquid medium (yeast nitrogen base without aminoacids, 6.7 g/L; raffinose 10 g/L; CSM without uracil and tryptophan at the proportions indicated by the supplier). The OD_{600nm} of this culture was measured, and cells were diluted in the same growth liquid media in order to be at the exponential growth phase in the following day (with a final OD_{600nm} around 1). OD_{600nm} of this second culture was measured, and the volume corresponding to an OD_{600nm} of 2 per mL was then centrifuged at 3000 rpm at 30 °C, for 4 min. The cells were washed in phosphate buffered saline (PBS) by resuspending them in this buffer and centrifuging again. Finally, the cells were resuspendend on PBS at a final OD600nm of 2 per mL ($\sim 3 \times 10^7$ cells per mL). Before loading the cells into the device, a vigorous vortex was made to avoid cell clusters.

D. Monitoring of Syn-GFP expression induction as a function of the local concentration of galactose

The measurement of the fluorescence in experiments involving cells was performed using an Axiovert 200 inverted fluorescence microscope (Carl Zeiss) and incorporated Axiocam MRm camera (Carl Zeiss), which was equipped to facilitate long-term maintenance of cells. Microscope and digital camera were controlled via AXIOVISION® software (Carl Zeiss). Syringe pumps were used, as described above, to insert fluids into the microfluidic structure. For cell loading, one syringe pumped SC raffinose 1% medium and the other the cell solution prepared as described above. For the formation of the gradient, in one inlet, SC galactose 1% liquid medium (GAL) was inserted, while in the other inlet, SC raffinose 1% liquid medium (RAF) was inserted.

The cell loading took 10 min with both pumps flowing at 0.5 μL/min.

A FOV of 400 × magnification was used to visualize the cell insertion process, which continued until approximately 60–80% of the traps were loaded with cells. Exposure times of 25, 50, 100, and 250 ms were used to minimize photobleaching. The fluorescence micrographs were analyzed using IMAGEJ® software. Because in some cases cells leaked from the traps, after image acquisition, the images were analyzed to find out which traps ensured a constant number of cells per trap throughout the duration of the experiment. The fluorescence intensity was determined in the area of homogeneous cell occupation in each trap along the microchannel.

III. RESULTS AND DISCUSSION

A. Generation of a stable GAL gradient inside of the microchannel

Fluid flow in microchannels is laminar so the streamlines are locally parallel and even obstacles in the flow are not expected to induce significant amounts of turbulence.[18,19] The microfluidic structures illustrated in Figure 2 were designed in AUTOCAD software and simulated using COMSOL software. As described above, "U"-shaped mechanical barriers (traps) were incorporated in the channel with the objective of achieving hydrodynamic cell immobilization along the channel and, subsequently, to allow monitoring of their behavior when submitted to biomolecular gradients. These traps have internal dimensions of $15 \times 10 \times 6\ \mu$m (volume of 0.9 pL).

Along the microchannel length of 2 cm, there are 19 sets of traps spaced 500 μm, each set containing 2 traps. The yeast cells used have a width of 4–8 μm and a length of 5–16 μm.

To study the formation of the gradient inside the microfluidic structure, water was pumped in both inlets of the "Y" at the same flow rate (0.5 μL/min). In one of the inlets, the solution contained 0.025 mol/m^3 of FITC. The concentration of FITC was monitored by fluorescence microscopy and used to characterize the diffusion process along the microchannel (Fig. 3). The flow (Navier-Stokes) and diffusion equations were solved using finite element methods. The calculated concentration profiles of FITC (assuming a diffusion coefficient $D = 5.2 \times 10^{-10}$ m^2/s) in the neighborhood of the 2nd, 9th, and 18th cell traps (respectively at 200, 900 and 1800 μm from the "Y" junction) are shown in Figure 3(a). The inlet with the FITC solution was on the left. Two observations can be made: (i) the further downstream the traps are, the more extensive is the FITC diffusion from the left to the right of the microchannel; (ii) the presence of a stagnant zone in the trap leads to an essentially flat FITC concentration at the entrance of the traps. The simulated concentration profile at the entrance of the traps is indicated with a full line in Figure 3(b) for the same set of traps. An analytical fit was made using $D = 5.2 \times 10^{-10}$ m^2/s and was compared to the normalized fluorescence intensity profiles across the channel.

The results of simulations were validated experimentally by fluorescence microscopy. Visually, the fluorescence intensities observed in the neighborhood of the 2nd, 9th, and 18th cell traps indicate that the FITC concentration is in qualitative agreement with the simulations [Fig. 3(a)]. In addition, the same kinetic behavior is observed with the experimental measurements, and the theoretical results at the entrance of the traps and along of the microchannel [Fig. 3(b)]. A steady state is obtained after a few seconds of flow. These results validate the hypothesis that it is possible to generate a desired concentration variation using the Y-shaped microfludic structure integrating U-shaped traps.

B. ASyn-GFP expression induction as a function of the generation of GAL and RAF gradients within microchannels

The microfluidic device was tested with genetically modified *S. cerevisiae* cells with the aim of understanding the effect of the establishment of a gradient of inducer (galactose) in the level of protein expression, in cells as a function of time and their position along the microchannel. The yeast strain VSY72 was used to visualize the expression levels of aSyn-GFP protein, having the encoding gene under the regulation of a galactose induced promoter, *GAL1*. Cells were pre-grown without galactose where aSyn-GFP protein is not expressed. The cells were then loaded into the device, as described above, and at time $t = 0$, GAL liquid medium was introduced into the left side of microchannel and RAF liquid medium into the right side of the microchannel [as indicated schematically in Figure 4(a)]. Figure 4(a) reviews graphically the present device concept with the two different solutions inserted in the microchannel from different sides (in this case, GAL solution on the left side) and the diffusion process along the Y-structure, exposing the cells trapped by hydrodynamic flow to a range of GAL concentrations.

The fluorescence intensity resulting from the aSyn-GFP expression of the cells distributed along the microchannel and positioned at the 2nd, 6th, 11th, and 17th sets of traps, as a function of time, was measured [Figs. 4(b) and 4(c)]. As expected, the further upstream the trap is located, the larger the difference in the measured fluorescence between cells on the GAL side and those on the RAF side. This is because, as discussed above, the closer the trap is to the inlet, the smaller is the extent of the galactose diffusion from the GAL to the RAF side of the microchannel. In traps further downstream, the fluorescence difference decreases due to increased diffusion. For example, for the 17th trap set, the fluorescence is essentially the same for traps on the GAL and RAF sides, indicating complete diffusion of the galactose across the width of the microchannel [Fig. 4(b)]. A clear increase of the fluorescence is observed for cells in all the traps between 2.5 and 4.5 h of exposure to the biomolecular gradient, indicating increasing levels of aSyn-GFP expression. At 6.5 h, fluorescence measured for the cells exposed to the highest concentrations of GAL saturates, suggesting that protein expression has reached

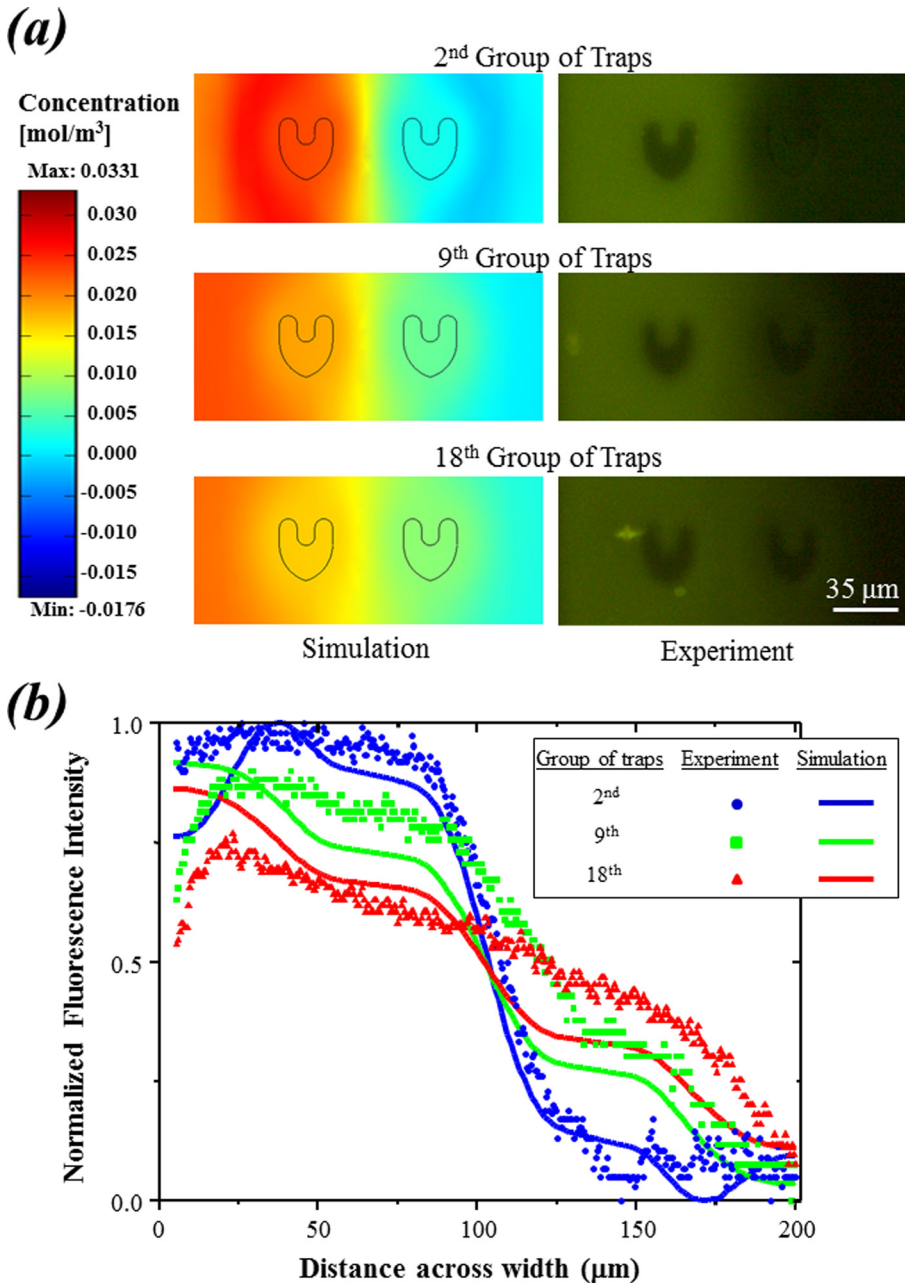

FIG. 3. Comparison of simulated and experimentally measured FITC gradients. (a) Left: simulated FITC concentration gradient flowing 0.025 mol/m^3 FITC concentration in one inlet and 0 mol/m^3 in the other, with a flow rate 0.5 μL/min in both inlets. Right: fluorescence micrograph of the microchannel at the indicated group of traps. (b) Comparison of the simulated and experimental results obtained. Results are representative of at least three independent experiments leading to similar results.

maximum values [Fig. 4(b)], as expected based on the aSyn-GFP expression profile determined by western blot (results not shown).

The previous fluorescence results were conjugated with a calculation of the galactose concentration at the same traps to produce a profile of the aSyn-GFP concentration (which is proportional to the measured fluorescence) as a function of the GAL concentration. In Figure 4(c), this profile is shown for 2.5 and 4.5 h after the establishment of the gradient in the microfluidic structure. The range of GAL concentrations accessible in this experiment was between 10 and 50 mM

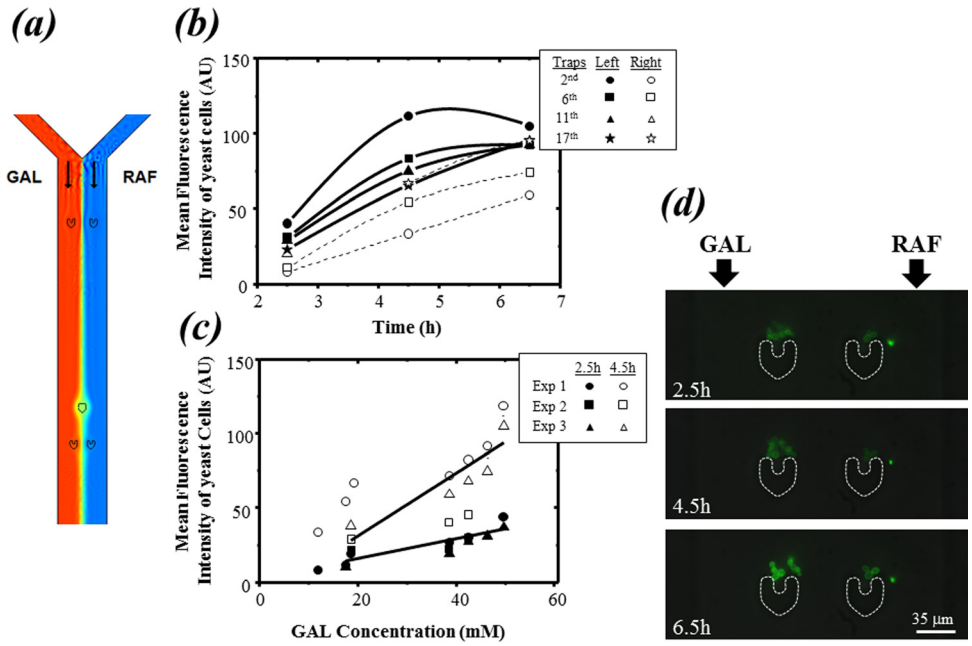

FIG. 4. Induction of aSyn-GFP expression as a function of the concentration of GAL (left insertion) and RAF (right insertion) in the microchannel. (a) Simulation of the microchannel and cell traps with GAL and RAF solutions forming a gradient. (b) The variation of mean fluorescence intensity in arbitrary units (AU) along the microchannel at the 2nd (●,○), 6th (■,□), 11th (Δ,▲) and 17th (open and close star) sets of traps, as a function of time. The closed symbols represent the left trap and open symbols, the right trap. (c) Measurement of the gradient evolution along the microchannel after 2.5 h (closed symbols) and 4.5 h (open symbols). The line is a linear regression. Results obtained for 3 independent experiments (Exp) are shown (indicated by the 3 different symbols). (d) Fluorescence micrograph series illustrating the variation of mean fluorescence intensity at the 6th set of traps of the yeast cells as a function of time, when exposed to concentration profiles along the channel defined for GAL medium and RAF medium; arrows show the flow direction; dashed lines indicate traps position. Results are representative of at least three independent experiments.

[Fig. 4(c)]. Moreover, protein expression levels in the cells are approximately linearly dependent on the GAL concentration (in the experimental range of concentrations) and increases with time [Fig. 4(c)]. Figure 4(d) shows a fluorescence micrograph series illustrating the variation of mean fluorescence intensity of the yeast cells as a function of time, when exposed to concentration profiles along the channel defined for GAL solution and RAF solution.

IV. CONCLUSIONS

The major conventional cell studies deal with large populations of cells, and consequently, measurements can only yield average values summed over the responses of many cells. However, this approach ignores the heterogeneity in cellular behaviour. In this sense, it is necessary to lead genetic, physiological, and biochemical cell studies on the scale of a single cell and with a sufficient number of cells in order to elucidate process heterogeneities and to obtain statistically meaningful data.[9]

The platform developed herein can be useful for these studies, as it allows control of the number of cells trapped and the possibility of monitoring single-to-few cells in a well established chemical microenvironment. Namely, a microfluidic device in which genetically modified yeast cells were hydrodynamically trapped in the presence of a steady-state biomolecular gradient was demonstrated. This microfluidic device was developed to enable single cell analysis where yeast cells express controlled levels a protein of interest. Here, the production of aSyn was obtained as a function of promoter-inducer concentration and time. Importantly, given the ease of use and reduced amounts of reagents required, the system described is amenable for high-throughput approaches. In addition, it combines flow cytometry and fluorescence microscopy features, allowing both the characterization of cell populations and the observation of

structures at the sub-cellular level. However, a major advantage over conventional methods is that microfluidic systems afford the possibility to follow the behavior of individual cells over time in a controlled and sustained environment. Our approach opens a wide range of possibilities for single cell analysis on this cell-based model of PD, which was developed as a living test tube for the study of aSyn biology and pathobiology.[11]

ACKNOWLEDGMENTS

The authors gratefully acknowledge M. Amaral for the early work on the gradients; V. Soares, F. Silva, and J. Bernardo for help in sample/cleanroom processing; M. Santos and P. Novo for PDMS support activities; José Rino and António Temudo for technical support. This work is supported by FCT through the Associated Laboratories IN and IMM. T.F.O. is supported by a Marie Curie International Reintegration Grant from the European Commission (Neurofold), and an EMBO Installation Grant. This work was supported by FCT through projects PTDC/SAU-NEU/105215/2008 and PTDC/CTM/104387/2008. S.T. is supported by FCT (SFRH/BPD/35767/2007).

[1]D. M. Thompson, K. R. King, K. J. Wieder, M. Toner, M. L. Yarmush, and A. Jayaraman, Anal. Chem. **76**, 4098 (2004).
[2]K. Sato, A. Hibara, M. Tokeshi, H. Hisamoto, and T. Kitamori, Anal. Sci. **19**, 15 (2003).
[3]F. K. Balagadde, L. You, C. L. Hansen, F. H. Arnold, and S. R. Quake, Science **309**, 137 (2005).
[4]R. M. Johann, Anal. Bioanal. Chem. **385**, 408 (2006).
[5]B. G. Chung, L. A. Flanagan, S. W. Rhee, P. H. Schwartz, A. P. Lee, E. S. Monuki, and N. L. Jeon, Lab Chip **5**, 401 (2005).
[6]F. Lin and E. C. Butcher, Lab Chip **6**, 1462 (2006).
[7]W. Saadi, S. J. Wang, F. Lin, and N. L. Jeon, Biomed. Microdevices **8**, 109 (2006).
[8]M. H. Wu, S. B. Huang, and G. B. Lee, Lab Chip **10**, 939 (2010).
[9]T. M. Keenan and A. Folch, Lab Chip **8**, 34 (2008).
[10]A. Seidi, H. Kaji, N. Annabi, S. Ostrovidov, M. Ramalingam, and A. Khademhosseini, Biomicrofluidics **5**, 22214 (2011).
[11]T. F. Outeiro and S. Lindquist, Science **302**, 1772 (2003).
[12]M. G. Spillantini, R. A. Crowther, R. Jakes, M. Hasegawa, and M. Goedert, Proc. Natl. Acad. Sci. U. S. A. **95**, 6469 (1998).
[13]I. Martin, V. L. Dawson, and T. M. Dawson, Annu. Rev. Genomics Hum. Genet. **12**, 301 (2011).
[14]D. W. Miller, S. M. Hague, J. Clarimon, M. Baptista, K. Gwinn-Hardy, M. R. Cookson, and A. B. Singleton, Neurology **62**, 1835 (2004).
[15]C. R. Scherzer, J. A. Grass, Z. Liao, I. Pepivani, B. Zheng, A. C. Eklund, P. A. Ney, J. Ng, M. McGoldrick, B. Mollenhauer, E. H. Bresnick, and M. G. Schlossmacher, Proc. Natl. Acad. Sci. U. S. A. **105**, 10907 (2008).
[16]E. Kim, Y. Xia, and G. M. Whitesides, Nature (London) **376**, 581 (2005).
[17]Y. Xia, E. Kim, X. M. Zhao, J. A. Rogers, M. Prentiss, and G. M. Whitesides, Science **273**, 347 (1996).
[18]J. Berthier, and P. Silberzan, *Microfluidics for Biotechnology* (Artech House, Boston, 2006).
[19]H. Bruus, *Theoretical Microfluidics* (Technical University of Denmark, 2004).